Journal of Physiology (1991), **436**, *pp.* 257–282
With 10 figures
Printed in Great Britain

REGULATION BY SYNAPSIN I AND Ca^{2+}–CALMODULIN-DEPENDENT PROTEIN KINASE II OF TRANSMITTER RELEASE IN SQUID GIANT SYNAPSE

BY R. LLINÁS*, J. A. GRUNER*†, M. SUGIMORI*, T. L. McGUINNESS‡, AND P. GREENGARD‡

*From the Marine Biological Laboratory, Woods Hole, MA, *Department of Physiology & Biophysics and †Department of Neurosurgery, New York University Medical Center, New York, NY and the ‡Laboratory of Molecular and Cellular Neuroscience, Rockefeller University, New York, NY, USA*

(*Received 3 August 1990*)

SUMMARY

1. Presynaptic or simultaneous pre- and postsynaptic voltage-clamp protocols were implemented in the squid giant synapse in order to determine the magnitude and time course of the presynaptic calcium current (I_{Ca}) and its relation to transmitter release before and after presynaptic injection of proteins. These included several forms of synapsin I, calcium–calmodulin-dependent protein kinase II (CaM kinase II) and avidin.

2. The quantities and location of these proteins were monitored by fluorescence video-enhanced microscopy during the electrophysiological measurements.

3. Presynaptic injection of dephosphorylated synapsin I inhibited synaptic transmission with a time course consistent with diffusion of the protein through the terminal and action at the active release zone. A mathematical model relating the diffusion of synapsin I into the terminal with transmitter release was developed to aid in the interpretation of these results.

4. Synapsin I inhibition of transmitter release was reversible.

5. The action of synapsin I was highly specific, as phosphorylation of the tail region only or head and tail regions prevented synapsin I from inhibiting release.

6. Injections of heat-treated synapsin I or of avidin, a protein with a size and isoelectric point similar to those of synapsin I, had no effect on transmitter release.

7. CaM kinase II injected presynaptically was found to facilitate transmitter release. This facilitation, which could be as large as 700% of the control response, was related to the level of penetration of the enzyme along the length of the preterminal. A mathematical model of this facilitation indicates a reasonable fit between the distribution of CaM kinase II within the terminal and the degree of facilitation.

8. The overall shape of the postsynaptic response was not modified by either synapsin I or CaM kinase II injection.

9. The data suggest that, in addition to releasing transmitter, calcium also penetrates the presynaptic cytosol and activates CaM kinase II. When activated, CaM kinase II phosphorylates synapsin I, which reduces its binding to vesicles

MS 8704

and/or cytoskeletal structures, enabling more vesicles to be released during a presynaptic depolarization. The amplitude of the postsynaptic response will then be both directly and indirectly regulated by depolarization-induced Ca^{2+} influx. This model provides a molecular mechanism for synaptic potentiation.

INTRODUCTION

Electrophysiological and morphological studies in the squid giant synapse preparation have yielded significant insights into the mechanisms of depolarization–release coupling in chemical transmission (Katz & Miledi, 1967; Llinás, Steinberg & Walton, 1981*a*, *b*; cf. Augustine, Charlton & Smith, 1987). Because both the pre- and postsynaptic terminals in this junction can be impaled directly (Bullock & Hagiwara, 1957; Hagiwara & Tasaki, 1958), the depolarization–release coupling process may be studied at its site of occurrence. We have recently examined some of the biochemical steps involved in the release process. Since the presynaptic terminal can generate action potentials (Miledi & Slater, 1966; Llinás, Sugimori & Simon, 1982), the effects of presynaptically injected proteins on depolarization–release coupling can be directly tested using spike activation. In addition, pre- and postsynaptic voltage clamping, combined with pharmacological blockade of Na^+ and K^+ conductances, allow precise measurement of the presynaptic Ca^{2+} current. Transmitter release can be inferred from the time course and amplitude of the postsynaptic potential (Llinás, Steinberg & Walton, 1976; Llinás *et al.* 1981*b*) or the postsynaptic current (Llinás & Sugimori, 1978; Augustine & Charlton, 1986), thereby allowing determination of the relationship between Ca^{2+} entry and transmitter release.

Several findings have suggested a prominent role for the protein synapsin I in synaptic transmission. For instance, synapsin I has been found to be nearly ubiquitous in presynaptic terminals, and to be closely associated with the cytoplasmic surface of small synaptic vesicles. It represents about 1% of the total neuronal protein in the mammalian brain (DeCamilli, Cameron & Greengard, 1983; Greengard, Browning, McGuinness & Llinás, 1987). Earlier experiments in the squid giant synapse have indeed shown that intracellular injection of synapsin I can block synaptic transmission, and that Ca^{2+}–calmodulin-dependent protein kinase II (CaM kinase II) has a facilitory effect (Llinás, McGuinness, Leonard, Sugimori & Greengard, 1985; Greengard *et al.* 1987).

Based on these and other findings, we hypothesized that synapsin I serves to immobilize synaptic vesicles by binding them to cytoskeletal elements, and that phosphorylation of synapsin I by CaM kinase II liberates vesicles from these attachments (Llinás *et al.* 1985; DeCamilli & Greengard, 1986; Greengard *et al.* 1987; McGuinness, Brady, Gruner, Sugimori, Llinás & Greengard, 1989; DeCamilli, Benfenati, Valtorta & Greengard, 1990).

The regulation of synapsin I phosphorylation is of central importance to this hypothesis. Synapsin I can be phosphorylated at three sites: site 1 is located in the globular head region of the molecule, while sites 2 and 3 are located in the elongated tail region. Previous studies have indicated that CaM kinase II is capable of phosphorylating synapsin I on its tail sites, while the head site can be phosphorylated either by cyclic AMP-dependent protein kinase or by Ca^{2+}–calmodulin-dependent

protein kinase I (Huttner & Greengard, 1979; Sieghart, Forn & Greengard, 1979; Huttner, DeGennaro & Greengard, 1981; Kennedy & Greengard, 1981; Czernick, Pang & Greengard, 1987; Nairn & Greengard, 1987). Phosphorylation of the tail region by CaM kinase II reduces the binding of synapsin I to synaptic vesicles (Huttner, Scheibler, Greengard & DeCamilli, 1983; Schiebler, Jahn, Doucet, Rothlein & Greengard, 1986; Benfenati, Bahler, Jahn & Greengard, 1989) as well as to actin (Bahler & Greengard, 1987; Petrucci & Morrow, 1987). It has been hypothesized that synapsin I cross-links synaptic vesicles to actin, and that upon phosphorylation of synapsin I by CaM kinase II, the vesicles are free to move from a 'reserve' pool to a 'releasable' pool (Llinás *et al.* 1985; Bahler & Greengard, 1987; Benfenati *et al.* 1989; DeCamilli *et al.* 1990). The size of the postsynaptic response would then depend on both the size of the inward calcium current and the number of vesicles available for release. Here we present results obtained following the injection of synapsin I and CaM kinase II which are consistent with this hypothesis. Some of the results have been reported in preliminary form (Llinás *et al.* 1985).

METHODS

Stellate ganglion preparation

Experiments were performed in the giant synapse of the squid *Loligo pealii* at the Marine Biological Laboratory, Woods Hole, MA, USA. After decapitation of the squid, the stellate ganglion was isolated from the mantle under running sea water and placed in the recording chamber. The connective tissue over its surface was removed while the ganglion was continuously superfused with artificial sea water for the duration of the experiment (Llinás *et al.* 1981*a*). The presynaptic terminal was impaled with two microelectrodes: one to inject current and the different proteins, and one to measure voltage, which provided the feedback signal for the voltage-clamp amplifier. Chemicals (TEA) and proteins (phosphorylated and dephosphorylated synapsin I, mock phosphorylated synapsin I, avidin and CaM kinase II) were injected into the presynaptic terminal, using pressure pulses 50–100 ms in duration, regulated to 10^5 N/m^2. The postsynaptic fibre was impaled with two electrodes, one for voltage recording, the other for current injection. A brief electrical stimulus to the presynaptic bundle via a bipolar electrode located proximal to the stellate ganglion was used to confirm the viability of the preparation prior to the initiation of each experiment. Following demonstration of synaptic transmission, the sodium and potassium conductances (g_K, g_{Na}) were blocked by bath application of tetrodotoxin (TTX; 5×10^{-6} M) and 4-aminopyridine (4-AP) (final concentration 1 mM). In addition, TEA was also injected presynaptically in some experiments (see Figs 6*A*, 9 and 10). Careful monitoring revealed that during this procedure the potential at the recording electrode depolarized transiently by 2–5 mV in successful injections. Only in those experiments where the membrane potential stabilized within 5 mV of the pre-injection membrane potential level was the experiment continued. In our initial experiments, dephosphorylated synapsin I was injected prior to any pharmacological intervention to investigate the action of synapsin I in the absence of the ionic channel blocker. The presynaptic as well as the simultaneous presynaptic and postsynaptic voltage-clamp and calcium current measurement techniques have been previously described (Llinás & Sugimori, 1978; Llinás *et al.* 1981*a*; cf. Augustine *et al.* 1987).

Visualization of intracellularly injected proteins

To visualize the proteins used in the presynaptic injections, the various forms of synapsin I and avidin were made fluorescent by conjugation to the dye Texas Red (see below). Binding of the dye to synapsin I did not alter its ability to: (a) be phosphorylated by CaM kinase II as assessed using the procedure of McGuinness, Lai & Greengard (1985); (b) bind to purified synaptic vesicles using the procedure of Schiebler *et al.* (1986); or (c) inhibit neurotransmitter release (present report). A high-gain fluorescence imaging system consisting of a Videcon camera attached to a microchannel plate-image intensifier (maximum light magnification, 10^6) allowed us to localize the protein in the

preterminal. The image was then analysed on a Hamamatsu C 1966 VIM image analysis system which gave a well-defined fluorescence profile. The movement of the labelled protein was measured at different times after the injection and its movement along the terminal was determined by entering the enhanced image into a computer for graphic analysis. The rate of protein movement was determined by measuring the advance of the wavefronts as the terminal filled, and then calculating the percentage area of the terminal which remained unfilled at each time point. As discussed below, after the protein had diffused several hundred micrometres and its concentration had declined, the wavefront became less well defined and thus its position gave an underestimate of the extent of protein movement into the terminal. The diffusion velocity of synapsin I and avidin measured in this way was typically 25–55 μm min^{-1} (cf. Fig. 3*C*).

The location of CaM kinase II was indirectly determined by adding Texas Red-labelled bovine serum albumin (BSA) to the injection solution since the binding of dyes interfered with its solubility and/or its ability to phosphorylate synapsin I. Addition of labelled BSA to the CaM kinase II solution had no detectable effect on the ability of the enzyme to phosphorylate synapsin I *in vitro* or on its ability to enhance neurotransmitter release from the giant synapse.

In early experiments the volume of synapsin I injected into the presynaptic terminal was determined using ^{125}I-labelled synapsin I which was measured directly, using a gamma counter. In five trials, the volume injected was 0·05–1 pl, i.e. $\leqslant$ 10% of the total volume of the terminal digit, corresponding to a maximal intracellular synapsin I concentration of 1·35 μM. Synapsin I, avidin and BSA had similar mobilities in the terminal.

Preparations of proteins

Dephosphorylated synapsin I was purified from bovine brain by modification (Bahler & Greengard, 1987) of the procedure of Schiebler *et al.* (1986). CaM kinase II was purified from rat forebrain as previously described (McGuinness *et al.* 1985), with the addition of hydroxylapatite chromatography inserted between the DEAE–cellulose chromatography and ammonium sulphate precipitation steps. The purified CaM kinase II (0·5 mg ml^{-1}) was dialysed extensively against 0·5 M-potassium acetate/10 mM-potassium phosphate, pH 7·4 (injection buffer) and stored at −70 °C until immediately before use. The catalytic subunit of cyclic AMP-dependent protein kinase, purified as described (Kaczmarek, Jennings, Strumwasser, Nairn, Walter, Wilson & Greengard, 1980), was a gift of Dr A. C. Nairn. Calmodulin was purified as described (Grand, Perry & Weeks, 1979). Avidin, a basic protein similar in size to synapsin I, was labelled with the fluorescent dye Texas Red. Texas Red-labelled avidin and Texas Red-labelled BSA were obtained from Molecular Probes (Eugene, OR, USA), dissolved in and dialysed extensively against the injection buffer, and stored in aliquots at −70 °C until immediately before use. Protein determinations were performed by the method of Peterson (1977) using BSA as the standard.

Synapsin I (0·35 mg ml^{-1}) was phosphorylated by incubation for 30 min at 30 °C in 50 mM-Tris-HCl, pH 7·5, 150 mM-NaCl, 0·4 mM-EGTA, 1 mM-dithioerythritol, 10 mM-$MgCl_2$, 100 μM-ATP with trace amounts of [γ-^{32}P]ATP, with either CaM kinase II (3·4 μg ml^{-1}), 0·7 mM-$CaCl_2$, 30 μg ml^{-1} calmodulin and/or the catalytic subunit of cyclic AMP-dependent protein kinase (60 nM/0·1% Nonidet-P40). Mock phospho-synapsin I was prepared as above except that both kinases, $CaCl_2$, calmodulin and Nonidet-P40 were added while ATP was omitted from the reaction mixture. Synapsin I was phosphorylated to a stoichiometry of 2·0 mol mol^{-1} by CaM kinase II and 0·95 mol mol^{-1} by the catalytic subunit of cyclic AMP-dependent protein kinase, as confirmed by one- and two-dimensional peptide mapping of the phosphorylated synapsin I molecules (Huttner *et al.* 1981; Kennedy & Greengard, 1981; Kennedy, McGuinness & Greengard, 1983).

The synapsin I preparations to be fluorescently labelled were dialysed extensively against 0·1 M-Tris-HCl (pH 9·0), 50 mM-NaCl and then concentrated on an Amicon centricon 30 unit to a final protein concentration of 1 mg ml^{-1}. Conjugation to the fluorescent probe Texas Red (Molecular Probes, Eugene, OR, USA) was performed according to the method of Titus, Haugland, Sharrow & Segal, (1982). Briefly, 1 mg of Texas Red was dissolved in 250 μl of dimethylformamide and an aliquot was immediately added to the protein solution (0·5–1·0 ml) using a ratio of 0·04 mg Texas Red: 1 mg protein. Conjugation reactions were carried out for 1 h at 4 °C. Synapsin I, in both the labelled and unlabelled preparations, was purified away from kinases and/or unbound Texas Red by CM–cellulose chromatography at pH 8·0 (Ueda & Greengard, 1977). Synapsin I was eluted from the CM–cellulose column with injection buffer, concentrated as described above, dialysed overnight against the injection buffer, centrifuged at 450000 *g* for 15 min to remove large aggregates, and

either stored at 0 °C and used within 7 days of preparation or stored at −70 °C and thawed immediately before use. The absorbance ratio $A_{596:280}$ of the labelled synapsin I ranged from 0·7 to 1·3, giving an estimated molar dye:protein ratio of 5:1 to 12:1. One-dimensional SDS-gel electrophoresis confirmed that the fluorescence co-migrated with the synapsin I protein staining bands.

Data analysis

Electrophysiological responses were stored on a Nicolet 4094B digital oscilloscope and transferred to a Macintosh II computer for analysis. Peak amplitudes for the postsynaptic potentials (PSP) or currents (PSI) were determined using the average value of the pre-stimulus baseline as reference. In some experiments, the amplitude of the postsynaptic response was obtained by integrating the curves over the period required for the largest response to return to baseline. Indeed, in those cases where the shape of the response curve did not change as a function of stimulus amplitude, the integral of the response was proportional to the peak response amplitude at all stimulus levels. This was tested in three preparations in which integrals of postsynaptic currents or voltage responses were calculated and compared to peak-to-peak amplitudes. In each case, there was a high ($R^2 \sim$ 0·95) linear correlation between the peak amplitudes and the integrals of the responses when compared at various stimulus levels, and there was no apparent change in the shape of the responses. The maximum rate of rise of the response was determined by a computer algorithm which determined slopes for successive sets of five points 20 μs apart, beginning at the onset of the stimulus artifact to the time of the response peak. The maximum slope determined by the computer was overlaid on the raw waveform for visual verification. Statistical calculations (linear correlation coefficients, t tests) were performed using commercial statistics programs.

RESULTS

The database comprised fifty-two experiments involving injections of various dephosphorylated and phosphorylated forms of synapsin I, avidin and CaM kinase II. The results of these experiments are summarized in Table 1. More than 100 experiments, in which the preterminal had been injected with one of the above proteins, were excluded from this database for one of the following reasons: (a) failure to achieve normal pre- and postsynaptic resting membrane potential values after injection; (b) significant drop in membrane potential (more than 5 mV) or of input resistance and (c) leakage of dye into the extracellular compartment. Fine adjustments of the electrode positions were sometimes needed to maintain recording integrity. If a microelectrode came completely out of a terminal more than once, the data were discarded.

Synapsin I and transmitter release

Effect of dephosphorylated synapsin I on neurotransmitter release elicited by presynaptic action potentials

In twenty-one experiments, dephosphorylated synapsin I (synapsin I) was successfully injected into the final preterminal digit between 200 and 1100 μm from its distal end and allowed to diffuse throughout the remainder of the digit. In one experiment the postsynaptic potential elicited by presynaptic nerve stimulation was measured at regular intervals after injection of the protein. This allowed the release properties of the synapse to be determined in the absence of other pharmacological agents. As shown in Fig. 1, injection of synapsin I was accompanied by a reduction of transmitter release as measured by the decline in amplitude of the PSP. The postsynaptic response decreased in amplitude after this injection as the protein

diffused into the preterminal digit, without any change in the amplitude of the presynaptic action potential. This decrease in the postsynaptic response was almost complete 24 min after the injection.

These findings are in agreement with our initial observations that the injection of dephosphorylated synapsin I can block the release of transmitter induced by

TABLE 1. Summary of injection experiments

Injection	*N*	NC	I	F
CaM kinase II	9	0	1	8
Synapsin I	21	1	20	0
Mock phospho-synapsin I*	3	0	3	0
Heat-treated synapsin I	2	2	0	0
Head–tail-phosphorylated synapsin I	4	3	1	0
Head-phosphorylated synapsin I	7	1	6	0
Tail-phosphorylated synapsin I	2	2	0	0
Avidin	4	4	0	0
Total number	52	—	—	—

N, total number; NC, no change; I, inhibition of release; F, facilitation.
* Prepared as phospho-synapsin I except *not* phosphorylated.

presynaptic action potentials (Llinás *et al.* 1985) and with those recently published on Mauthner cell function in the vertebrate central nervous system (Hackett, Cochran, Greenfield, Brosius & Ueda, 1990).

Relation between dephosphorylated synapsin I diffusion into the terminal and neurotransmitter release evoked by presynaptic voltage steps

In order to establish the parameters that determine blockade of transmitter release by dephosphorylated synapsin I, calcium currents were measured before and at several intervals after injection of synapsin I. The presynaptic terminal was voltage clamped and transiently depolarized by rectangular voltage pulses of constant amplitude (40 mV) and duration (4·5 ms) from a holding potential of −65 mV. This allowed the time course and amplitude of the postsynaptic response to be determined as a function of the presynaptic I_{Ca} (Llinás *et al.* 1981*a*, *b*; Augustine, Charlton & Smith, 1985).

The decrease in postsynaptic response to constant amplitude voltage steps following synapsin I injection at the proximal end of the presynaptic digit is shown in Fig. 2. The presynaptic voltage step was repeated at the intervals indicated by the numbers to the left in the top panel of Fig. 2 which indicate time in minutes after injection. The results confirm our previous finding that synapsin I does not affect I_{Ca}, in contrast to its dramatic inhibition of the postsynaptic response (Llinás *et al.* 1985). Almost complete inhibition of the postsynaptic response occurred at about 25–30 min (see plot in Fig. 3*B*). In this experiment, g_K was not completely blocked, as TEA was not injected to avoid a possible interaction with the action of synapsin I. However, it can be seen that the initial rate and amplitude of I_{Ca} was unaffected by synapsin I. Furthermore, in subsequent experiments (see Fig. 6) it was observed that TEA, in amounts required to abolish the K^+ currents, did not interfere with the ability of synapsin I to block transmitter release.

In order to determine the mobility of synapsin I within the presynaptic cytosol, and to investigate the relationship between the location of synapsin I and transmitter release, a series of experiments were carried out in which synapsin I was injected at various locations along the preterminal. Synapsin I was labelled with the fluorescent

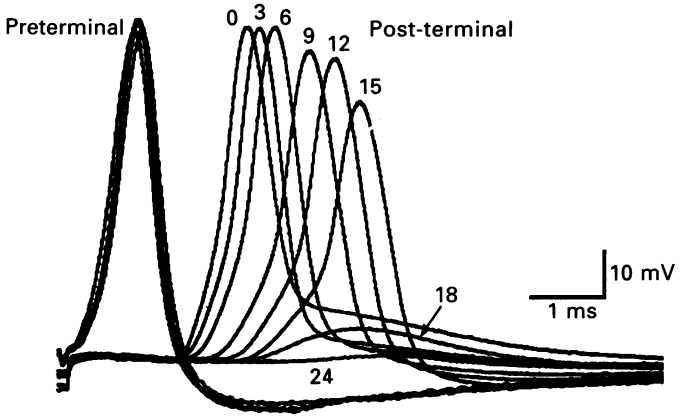

Fig. 1. Pre- and postsynaptic potentials from the squid giant synapse before and after presynaptic injection of synapsin I. Synaptic transmission was almost completely blocked 24 min after injection. No significant change in the presynaptic spike was observed. The decrement in postsynaptic spike amplitude was due to g_{Na} inactivation and g_K activation as the time required for the PSP to reach firing level was prolonged by the progressive block of synaptic transmission. The numbers give the time after synapsin I injection in minutes.

dye Texas Red and imaged using video-enhanced microscopy (see Methods) which allowed constant monitoring of the diffusion of the synapsin I–Texas Red conjugate. The results of two experiments are shown in Fig. 3. The initial diffusion rate of synapsin I into the presynaptic terminal, as determined by analysis of video-enhanced microscopic images of five individual injections, ranged between 23 and 108 μm min^{-1} (mean $\pm$ S.D. = 54 $\pm$ 33). This value is similar to that found for injection of similar proteins, such as avidin (see below). The amplitude of the postsynaptic response and the filling of the presynaptic terminal are plotted in Fig. 3*A* as a function of time for a synapse in which synapsin I was injected 300–400 μm proximal to the beginning of the synaptic zone region. Data for a synapse in which the injection was near the proximal edge of the active zone region are plotted in Fig. 3*B*. The maximal reduction in mean amplitude occurred after synapsin I had completely filled the presynaptic terminal (Fig. 3*B*).

The initial rate of filling of the presynaptic terminal was best fitted by a linear function. In cases where the injection was relatively small and/or more than several hundred micrometres from the end of the terminal, the fluorescence intensity became faint and the diffusion rate appeared to slow dramatically near the end of the terminal. In Fig. 3*B*, for example, the fluorescence was very low after the initial 5 min following injections. This did not occur for the injection shown in Fig. 3*A*, perhaps because of the relatively large size of the injection.

In contrast to the linear time course of filling of the terminal, the initial time course of postsynaptic inhibition was better fitted by an exponential curve. When the injection was further from the edge of the active zone, as in the experiment illustrated in Fig. 3*A*, the onset of inhibition was delayed for a period of time. In

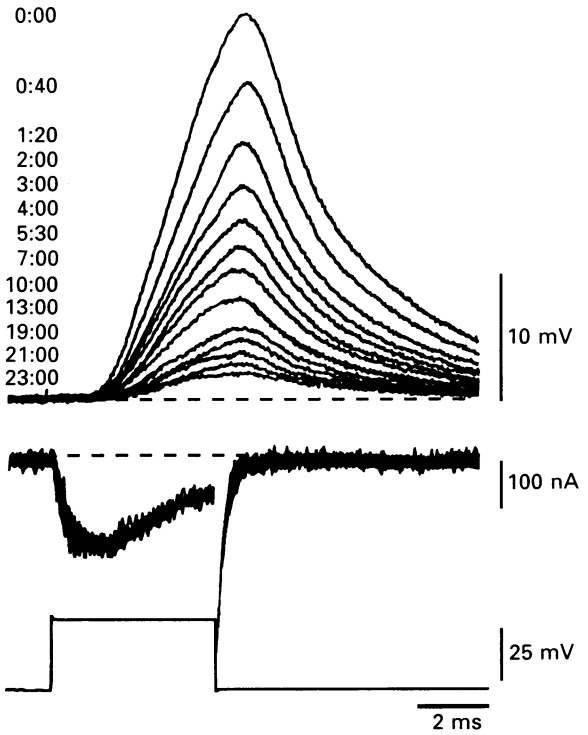

Fig. 2. Postsynaptic voltage (above) and presynaptic I_{Ca} (middle) following a presynaptic injection of synapsin I. A constant presynaptic voltage pulse was delivered at regular intervals before and after the injection (bottom). The postsynaptic responses illustrated were recorded at the intervals given by numbers to the left (in minutes).

some cases, the rate of reduction in PSP amplitude also appeared to decline as the wavefront approached the end of the terminal, suggesting that release from the most distal terminal region may not be as large as that from the rest of the preterminal.

Since the morphology of the preterminal varies quite markedly in length, position and diameter (Martin & Miledi, 1986), drawings were made of the terminals in all experiments in which dye-labelled proteins were injected. The amplitude of the postsynaptic potential is plotted as a function of time after synapsin I injection in Fig. 4 for five terminals (including those shown in Fig. 3) along with diagrams showing the movement of the dye through the terminal digit. The approximate position of the active synaptic release zone, as determined by microscopic observation, is indicated in Fig. 4*B*. Two injection sites were at the release zone; one was on the proximal edge, and two were several hundred micrometres distant from the proximal edge of the active zone. When synapsin I was injected at the *centre* of

the digit and the diffusion distance to the release sites was negligible, the blockade occurred almost immediately (up to 80% reduction within 1 min) in most cases. In such cases, presynaptic filling and complete blockade could occur in as little as 3–5 min, and the time to complete blockade was closely related to the time taken to

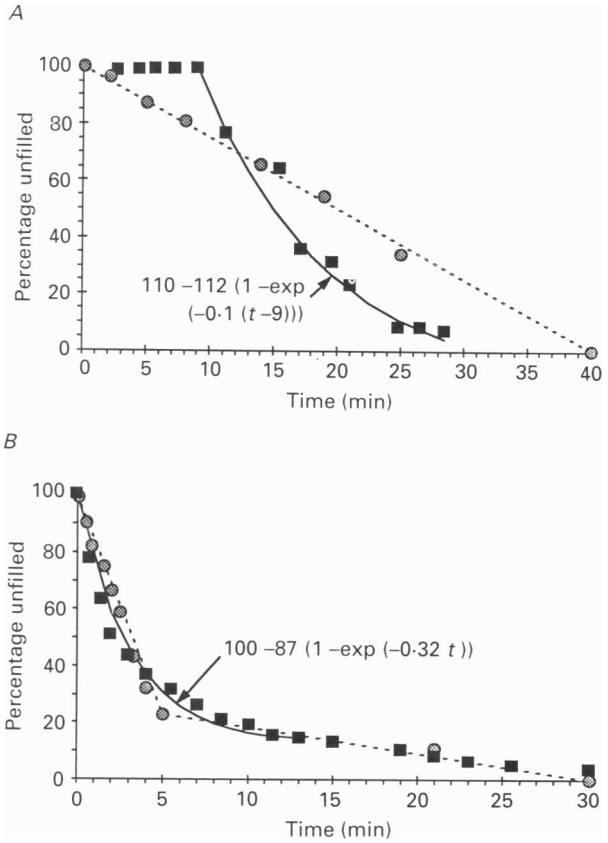

Fig. 3. Comparisons of the time course of PSP amplitude and terminal loading with Texas Red-labelled synapsin I, as determined by movement of the fluorescent wavefront. *A*, injection 300–400 μm from the proximal edge of the synaptic zone. Note linear filling of terminal by label (⊗). PSP amplitude began to decline exponentially about 10 min after synapsin I injection (■). *B*, injection near the proximal edge of the synaptic zone. Movement of label was initially linear, then slowed after 5 min while it diffused through the last third of the terminal (⊗). PSP amplitude began to decline immediately after injection, initially following an exponential time course, then becoming more linear after 10 to 15 min (■).

fill the entire terminal as determined by video analysis. In some cases the inhibition of transmitter release did not begin for up to 2 min after the injection, even in cases where synapsin I was deposited at the centre of the active zone region as, for example, injection no. 2 in Fig. 4. This small delay might be related to the size of the injections. Thus, in the case of injection no. 2, which was smaller than usual, diffusion to the release zone may have been prolonged.

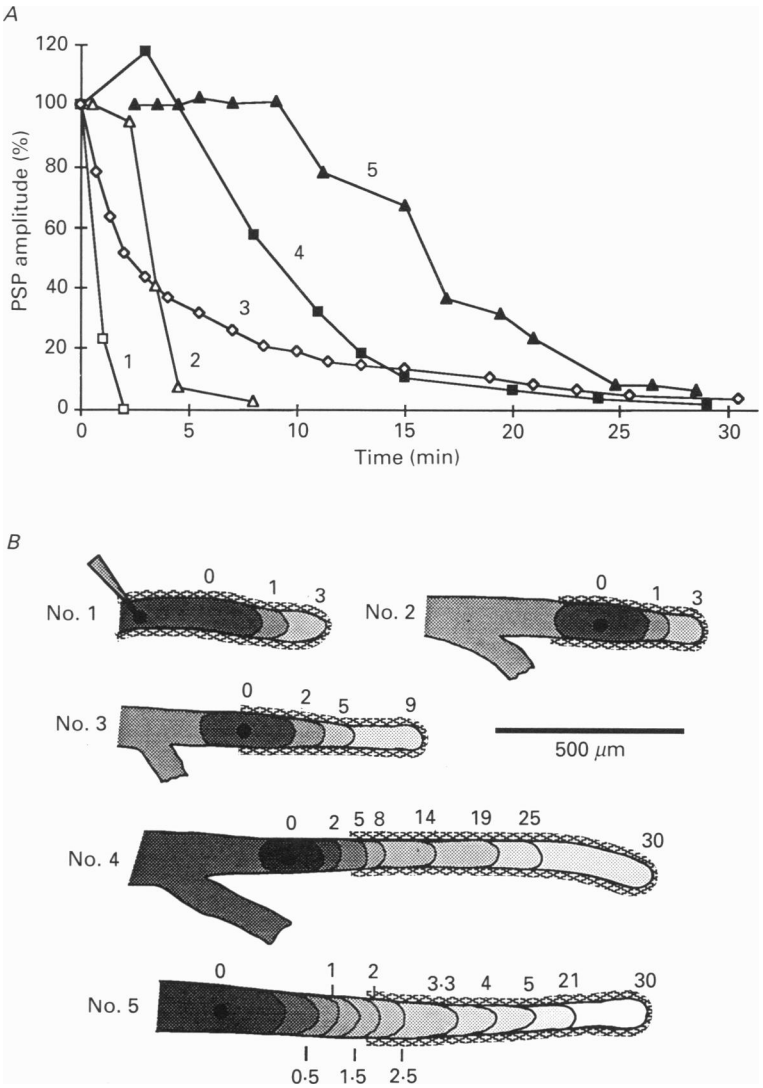

Fig. 4. Synapsin I loading and PSP amplitude. *A*, plot of PSP amplitude (as a percentage of pre-injection peak amplitude) as a function of time for five synapsin I injections at different points along the terminal finger as shown in *B*. Note progressively delayed onset and lower rate of inhibition when injection was farther from the end of the digit. *B*, reconstructions of terminals from video images showing the progression of the fluorescent wavefront at times (in minutes) indicated after injection. The electrode tip is indicated by black dot. Note that at $t = 0$, the volume of labelled synapsin I injected is indicated by the size of the region immediately surrounding the injection site. The location of the junction is indicated by the stippled pattern around the outside. The injection numbers (nos. 1–5) appear to the left of the reconstructions. Injections nos. 1 and 2 were within the active zone; no. 3 was near the proximal edge; and nos. 4 and 5 were approximately 200 and 400 μm proximal to the edge, respectively.

When synapsin I was injected close to the proximal border of the active zone area (injection no. 3), inhibition began within 1–2 min, but the time required for complete inhibition was longer, presumably because the protein had to travel farther to penetrate the entire terminal. As seen in Fig. 3*B*, and in Fig. 4 injection no. 3, 80% inhibition took 10 min to occur in this case. When synapsin I was injected several hundred micrometres from the terminal digit, a delay of 3–10 min was seen between injection and onset of blockade. In Fig. 4 injection no. 5 (300–400 μm from the active zone), synapsin I was not detected at the active zone until about 15 min after injection, while inhibition began at approximately 10 min. This temporal disparity may be accounted for by differences in threshold for visual detection *versus* synaptic inhibition, as discussed below.

Theoretical model for synapsin I action on synaptic transmission

In order to better understand the dynamics of terminal filling and PSP blockade, we developed a compartmental model for the diffusion of synapsin I into the presynaptic terminal in which n equal dimension compartments were placed end to end, and several compartments in the centre were filled with dye (or protein) at time 0 ($t = 0$). The fluorescent dye was then allowed to 'diffuse' through the compartments (Fig. 5). According to Fick's First Law of Diffusion

$$S_{ix} = -D_i \frac{\partial c_i}{\partial x},$$

where S = solute flow of the ith particle as a function of distance x, D = the diffusion coefficient, and c = concentration, the amount of dye diffusing between two compartments will depend on the difference in concentration between them. This is equivalent to assuming that at each time point, a fixed percentage ('D') of the dye in each compartment will move to either of the adjacent compartments. Here we have used a compartmental model, assuming for convenience that at each time point some percentage of the dye in each compartment, j, will move into each of the adjacent compartments, i.e.

$$c_{j,t} = (1-2D)\,c_{j,t-1} + D(c_{j-1,t-1} + c_{j+1,t-1}), \tag{1}$$

where $c_{j,t}$ is the concentration of protein in compartment j at time t, and D is the 'diffusion coefficient' of the dye (here chosen to be 0·25).

The right-most compartment was closed to simulate the end of the terminal. To simulate the injection corresponding to the data shown in Fig. 3*A*, fourteen compartments 'distal' to the injection site at C_0 were used, with C_0 and the compartment on either side filled with 1000 units of dye at time 0.

Figure 5 shows the results of this simulation for the compartments C_n, where $n = -14$ to 14, from $t = 0$ to $t = 50$. As the dye moves through the terminal, the concentration in each compartment rises, but progressively more slowly with distance as the concentration gradient decreases along the terminal. Curve C_{13} is closer to C_{14} than to C_{12} because C_{14}, being the last compartment, only loses dye to C_{13}. The initial time of appearance of dye in each compartment is a linear function (indicated by the descending dashed line) since the diffusion rate at any point is

constant and independent of concentration. However, if there is a detection threshold for the fluorescence, say 1 unit (0·1% of the initial injection; horizontal dashed line), then beginning with compartment C_7, the diffusion rate of the dye will appear to slow significantly. Thus, between C_7 and C_{14}, the distances (times) between

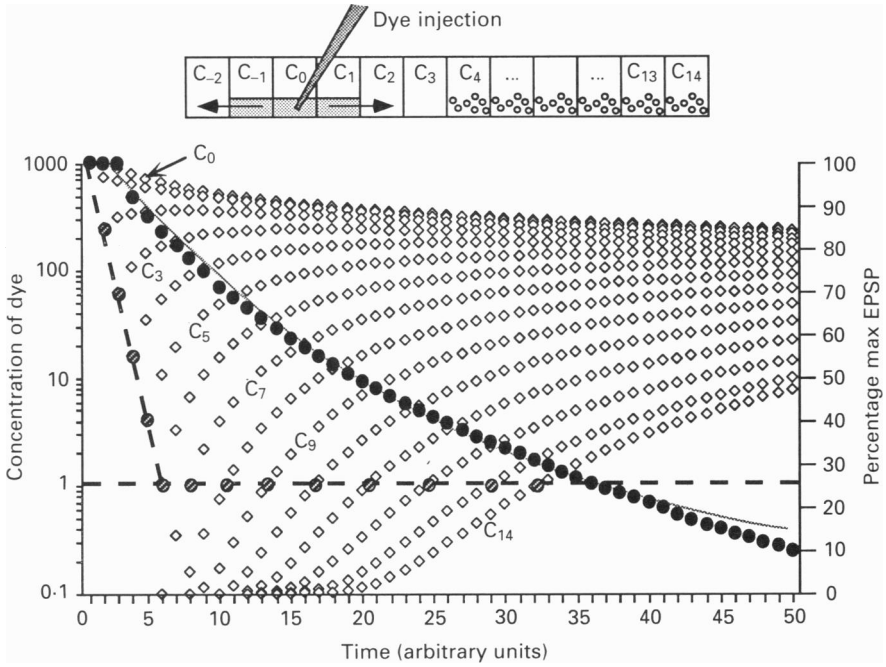

Fig. 5. Compartment model of diffusion of synapsin I along interior of the squid axon. The model consisted of twenty-nine compartments (C_{-14}–C_{14}; C_{-14}–C_{-3} not shown). The model illustrates the diffusion of synapsin I with respect to time in compartments C_0 (the centre of the 'injection') to C_{14} (the end of the terminal). The 'synaptic release zone' consisted of compartments C_4–C_{14}, each of which contained 1000 unbound 'vesicles.' A diffusion constant of 0·33 was assumed, with $k_3 = 300$. Curves marked with ◇ show the concentration of synapsin I (in arbitrary units) for compartments C_0 through C_{14} as a function of time after injection. Horizontal dashed line is hypothetical level for dye detection. The dye detection threshold generates a delay in visual detection of the dye in compartments C_7–C_{14} due to slow accumulation of dye (◉). ● illustrate the theoretical decline of PSP amplitude in the presence of synapsin I.

the intersections of the horizontal threshold line and the concentration–time curves increase. These results are qualitatively consistent with the observed diffusion rate of labelled synapsin I, particularly the apparent slowing of the diffusion rate near the terminal end as in Fig. 3*B*.

Since the model for diffusion of synapsin I appeared to describe correctly the principal features of the dye movement, it was then expanded in an attempt to model the effects of synapsin I on transmission. This model, based on eqns (2) to (5) below, is based on the following assumptions. (a) The response amplitude (R) for a given stimulus is proportional to the sum of the vesicles released from all compartments

(eqn (2)). (b) The number of vesicles released from each compartment (N_{jR}) is proportional to the number of free vesicles in that compartment (N_{jF}) (eqn (3)). (c) The number of free vesicles in a given compartment equals the number in the starting pool at time 0 (V_0) less the number bound (N_{jB}) by synapsin I per compartment (eqn (4)). (d) The number of bound vesicles is proportional to the concentration of active (dephosphorylated, D) synapsin I (S_j^D) in a given compartment (j) (eqn (5)) (k_1, k_2 and k_3, are constants):

$$R = k_1 \sum_{j=-n}^{j} N_{jR}; \tag{2}$$

$$N_{jR} = k_2 N_{jF}; \tag{3}$$

$$N_{jF} = V_{0,j} - N_{jB}; N_{jF} \geqslant 0; \tag{4}$$

$$N_{jB} = k_3 [S_j^D]. \tag{5}$$

These equations reduce to eqn (6):

$$R = k_1 k_2 \sum_{j=-n}^{n} V_0 - (k_3 [S_j^D]) \tag{6}$$

The diffusion parameter D, the constant, k_3 (which presumably corresponds to the 'activity' of dephosphorylated synapsin I in terms of vesicle binding), the size and location of the injection (1000 units of synapsin I injected into each of compartments C_{-1}, C_0, and C_1), and the size of the active zone (compartments C_4 through C_{14}, each containing 1000 vesicles) were chosen to simulate the data of injection no. 4 (Fig. 4). For simplicity, we have assumed that the product of the constants $k_1 k_2 = 1$ in this simulation. The constant k_3 was then adjusted to produce approximately 90% inhibition at the final time point. The shape of this curve is neither linear nor exponential, as shown by superimposing an exponential curve whose parameters were adjusted to match the initial decline of the inhibition curve. In fact, as 'inhibition' proceeds, the curve becomes increasingly linear, precisely as seen with injections nos. 3, 4 and possibly 5. An important feature of the model which contributes to the changing rate of inhibition seen in this curve is the assumption that the number of free vesicles cannot be less than zero (eqn (4)). Thus when all vesicles in a compartment are bound, it cannot contribute further to inhibition.

Reversibility of synapsin I reduction of neurotransmitter release

In most experiments a rapid and profound block of synaptic transmission followed synapsin I injection, indicating that the release mechanism was totally overwhelmed. It was assumed that injection of a smaller amount of synapsin I might allow a recovery of synaptic transmission. This experiment would also serve as a test for any possible deleterious effects of the synapsin I injections on transmitter release *per se*.

As illustrated in Fig. 6, recovery of transmitter release was observed when a smaller amount of synapsin I was injected in a synapse which remained in excellent condition for 90 min after the injection. The pre-injection responses for a set of depolarization steps are shown in Fig. 6*A* and *B*. Similar sets of presynaptic pulses

were generated 12, 25 and 75 min later. In each case the corresponding presynaptic calcium currents (Fig. 6*A*) were comparable to the controls. The postsynaptic responses, which were markedly reduced at 12 and 25 min, recovered to nearly normal levels by 75 min. The plot of peak PSP amplitudes for each stimulus level as a function of time after injection (Fig. 6*B*) showed that recovery began between 12 and 25 min after the injections.

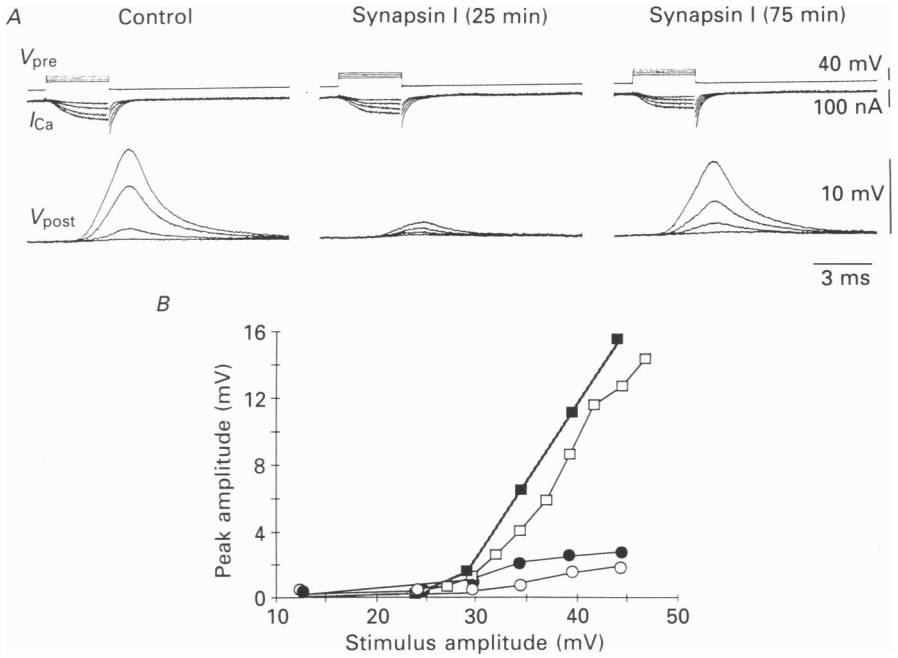

Fig. 6. Reversibility of synapsin I inhibition of neurotransmitter release. *A*, time course of recovery of transmission after synapsin I injection. Four presynaptic voltage-clamp steps (upper) were delivered at each time interval which resulted in a graded series of Ca^{2+} current (middle) and PSP (lower) responses. Postsynaptic responses were strongly depressed at 25 min compared to pre-injection responses, while presynaptic Ca^{2+} current was unaffected. PSP amplitudes recovered to near-normal levels by 75 min. *B*, plot of peak PSP values as a function of voltage-step amplitude showing maximum inhibition at about 12 min. ■, 0 min; ○, 12 min; ●, 25 min; □, 75 min.

Injection of phosphorylated synapsin I into the presynaptic terminal

Further experiments were designed to test the effect of phosphorylation of the various sites of synapsin I on its ability to affect transmission. Samples of phospho-synapsin I (in which only the head region or only the tail region, or both, were phosphorylated) were prepared and injected into a number of synapses (see Table 1).

Two examples of results from each type of injection are shown in Fig. 7. In the cases of synapsin I phosphorylated in the head and tail regions (head–tail-phosphorylated synapsin I; Fig. 7*A*), or synapsin I phosphorylated only in the tail region (tail-phosphorylated synapsin I; Fig. 7*B*), the injection had no effect on synaptic transmission. The slight increase after the injection and gradual reduction

of the synaptic response in the case of one tail-phosphorylated synapsin I injection (upper curve, Fig. 7*B*) was similar to responses seen in some control experiments where either avidin or heat-treated synapsin I was injected (see below). In contrast, transmission was inhibited by synapsin I phosphorylated only in the head region

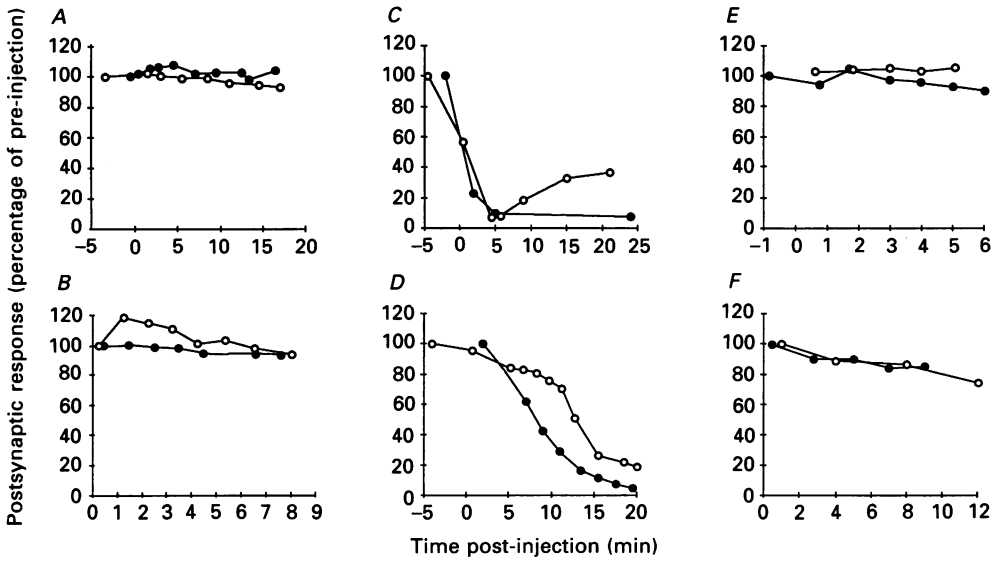

Fig. 7. Results of presynaptic injection of various phosphorylated forms of synapsin I. Two experiments are shown for each type of injection. Note that head and tail phosphorylation (*A*) or tail-only phosphorylation (*B*) of synapsin I prevented inhibition, while head phosphorylation (*C*) did not. *D*, injection of 'mock' phospho-synapsin I (prepared as head–tail-phosphorylated synapsin I except for the omission of ATP from the phosphorylation reaction) blocked transmission. Injections of heat-treated synapsin I (*E*) or avidin (*F*) did not affect transmitter release. Data are plotted as a percentage of pre-injection PSP amplitude.

(head-phosphorylated synapsin I; Fig. 7*C*). Note that there was some recovery from inhibition in the case of one of the head-phosphorylated synapsin I injections, indicating a reversible action as shown for dephosphorylated synapsin I in Fig. 6. In all of the cases illustrated in Fig. 7, the I_{Ca} was unchanged by the protein injection (not shown).

Since the ineffectiveness of some of the phosphorylated forms of synapsin I could have been due to inactivation of the protein during the phosphorylation reaction, it was felt that an additional control for the negative results with the phosphorylated forms of synapsin I was required. For this reason, 'mock' phospho-synapsin I was prepared (see Methods) in which both enzymes necessary for phosphorylating both the head and tail regions were present, but ATP was omitted to prevent actual phosphorylation. In this case, inhibition of transmission was observed exactly as seen with conventionally prepared synapsin I (Fig. 7*D*).

In summary, the results of injections of the phosphorylated forms of synapsin I confirmed our initial findings that phosphorylation of the tail region of synapsin I

abolishes its ability to block synaptic release (Llinás *et al.* 1985). Phosphorylation of the head region does not influence the inhibitory ability of synapsin I, nor does it reverse the effect of tail phosphorylation.

Injections of heat-treated synapsin I and of avidin

It was previously determined that heating the synapsin I molecule abolishes its ability to block synaptic transmission (Llinás *et al.* 1985). Examples of two such injections are shown in Fig. 7*E*. As an additional control for certain physical properties of synapsin I, Texas Red-labelled avidin was injected. Avidin is a protein which has a size ($M_r = 63000$) and pI (10·6) similar to those of synapsin I. These experiments were performed in a manner similar to those described for synapsin I. The postsynaptic response as a function of time after two avidin injection experiments is shown in Fig. 7*F*, which indicates little or no effect on transmission. The relationship between the postsynaptic response and the diffusion of avidin as reconstructed from video analysis for one of these injections is shown in Fig. 8. The diffusion rate was similar to that of synapsin I, ranging between 23 and 54 μm min^{-1} (mean $\pm$ S.D. = 39 ± 12; $n = 4$). Avidin had no effect on transmitter release even when monitored up to 30 min after injection, at which time the fluorescence was relatively evenly distributed throughout the terminal. Note in the experiment illustrated in Fig. 8*C* that the diffusion rate for avidin is nearly constant along the entire length of the terminal.

CaM kinase II and transmitter release

Injection of CaM kinase II

The previous set of experiments indicated that synapsin I in its dephosphorylated form blocked synaptic transmission while tail-phosphorylated synapsin I had no effect. Further studies were designed to test the hypothesis that CaM kinase II acts to modulate the synapsin I-dependent binding of synaptic vesicles to the intracellular matrix. If the enzyme dissociates vesicles from their attachments by phosphorylating an endogenous synapsin I-like molecule, increasing the endogenous CaM kinase II normally present in the terminal should increase transmitter release. In our preliminary study in the squid synapse, the injection of CaM kinase II markedly facilitated transmitter release without significantly modulating the presynaptic Ca^{2+} current in each of three experiments (Llinás *et al.* 1985). The diffusion rate of CaM kinase II was not directly assessed because labelling with any of the usual dyes was found to interfere with its solubility and/or ability to phosphorylate synapsin I.

In the present study injection of of CaM kinase II was followed by facilitation of transmitter release in all but one experiment. In eight out of nine experiments, transmitter release was facilitated after the injection of CaM kinase II as shown for one synapse in Fig. 9. Blockage of transmission was seen in one experiment, although there was no obvious damage to the synapse. In five experiments which were analysed quantitatively, the mean per cent facilitation was 409 ± 157 %. The maximal facilitation usually occurred between 10 and 20 min after injection. Presynaptic voltage steps of different amplitudes were applied to the presynaptic terminal while employing a double voltage clamp to determine I_{Ca} and postsynaptic

current (I_{post}). The double voltage clamp was preferable in order to prevent the postsynaptic potential from reaching the PSP reversal potential during facilitation by CaM kinase II, which would result in response saturation.

A double voltage-clamp experiment showing facilitation following CaM kinase II injection is illustrated in Fig. 9. The time course and amplitude of I_{post} (post-injection

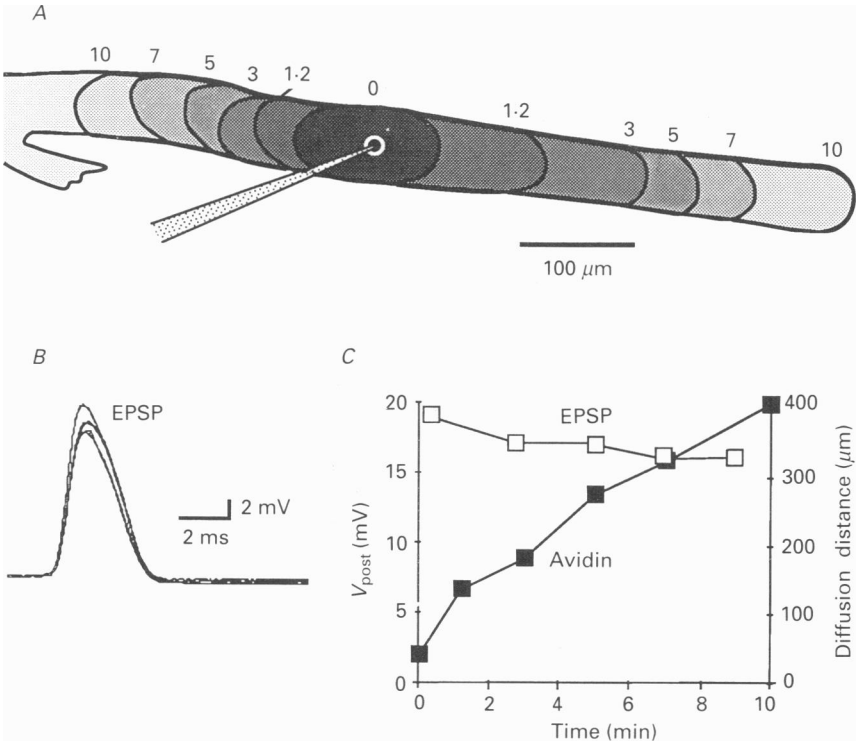

Fig. 8. Effect of injection of Texas Red-labelled avidin on synaptic transmission. *A*, diffusion of dye along synaptic digit as a function of time (numbers above drawing; in minutes), as determined by enhanced image from the video monitor. Black dot marks electrode tip; immediately surrounding stippled area is volume filled after initial injection. *B*. PSPs between 0 and 10 min following avidin injection showing this protein had a minimal effect on the PSP. *C*, plot of diffusion distance and PSP amplitude as a function of time showing linear avidin diffusion rate and minimal effect on transmission.

current) for three different times and levels of presynaptic depolarization are shown. Following CaM kinase II injection, the PSP was facilitated as early as 2 min post-injection, and increased in amplitude by over 600 %. This facilitation was associated with a corresponding increase in the rate of rise in I_{post} for a given level of I_{Ca}. In Fig. 9*C*, the postsynaptic current increased to the point of saturation, as evidenced by the flattened top of the response. Note that, in this experiment, the amplitude onset kinetics (Llinás *et al.* 1981*a*, *b*) and the tail component of the macroscopic inward calcium current were not modified by CaM kinase II. Moreover, these currents were similar to those previously reported in the absence of CaM kinase II (Llinás *et al.* 1981*a*, 1982; Augustine *et al.* 1985). Figure 10 illustrates the relative enhancement

of the PSP and PSI following CaM kinase II injection for four experiments. The actual ranges of PSP and PSI amplitudes for each experiment are noted at the right. Data from three experiments overlap, while one synapse had a more delayed and slower rising facilitation. Exponential curves were then empirically fitted to this range of data (thin continuous lines).

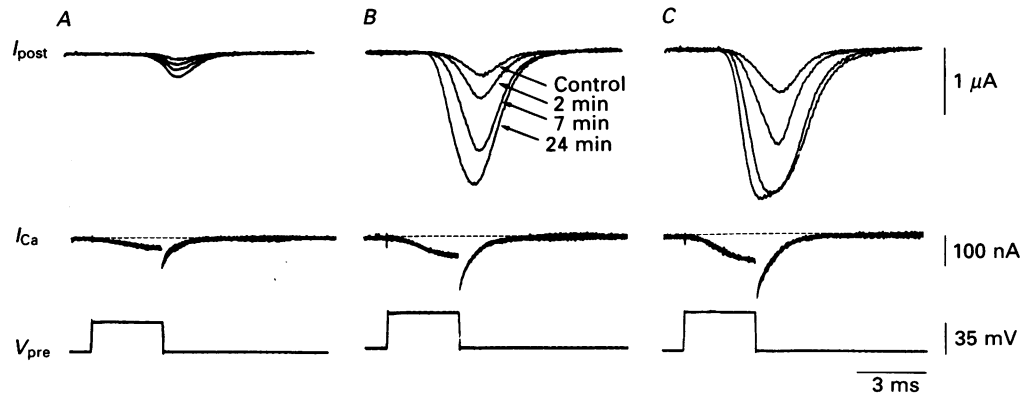

Fig. 9. Recordings showing time course of facilitation of synaptic transmission after CaM kinase II injection into the presynaptic digit. *A*, *B* and *C*; postsynaptic currents (upper traces) in response to 25, 30 and 35 mV presynaptic voltage-clamp steps (lower traces). Responses to each step were recorded before and at the three times after the injection noted in *B*. Note that I_{Ca} (middle traces) at each stimulus level was constant over time. At the highest stimulus level (*C*), postsynaptic response saturation occurred at 24 min.

Theoretical model for CaM kinase II action on synaptic transmission

If the hypothesis is correct that CaM kinase II acts on neurotransmitter release by regulating the phosphorylation state of synapsin I, then the model of vesicle release presented above should also apply to the facilitation produced by CaM kinase II. In particular, k_3 can be considered to be related to the degree of phosphorylation and inactivation of synapsin I by CaM kinase II. Starting with eqn (6) above, we may assume that the ratio of the concentrations of the phosphorylated to dephosphorylated synapsin I ($[S^P]/[S^D]$) is directly proportional to the concentration of CaM kinase II ([CK]), i.e.

$$\frac{[S^P]}{[S^D]} = k_4[CK], \tag{7}$$

where k_4 is a constant. Equation (6) can then be rewritten with respect to the individual compartments (j):

$$R = k_1 k_2 \sum_{j=-n}^{n} V_0 - \frac{k_3[S^T]_j}{1+k_4[CK]_j}, \tag{8}$$

where $[S^T]_j$ is the total phosphorylated plus dephosphorylated synapsin I in each compartment.

To simulate an injection of CaM kinase II, eqn (1) was used to model diffusion of CaM kinase II through the terminal, with S^T set to a constant value in each

compartment. The parameters of the model (eqn (8)) were then adjusted to produce a curve which fell roughly in the centre of the range of experimental data. These values are shown as a thick line in Fig. 10. The specific parameter values were: $k_1 = k_2 = 1$, $S^T = 10000$, $k_3 = 1$, and $k_4 = 0{\cdot}0002$. The value of [CK] was set to

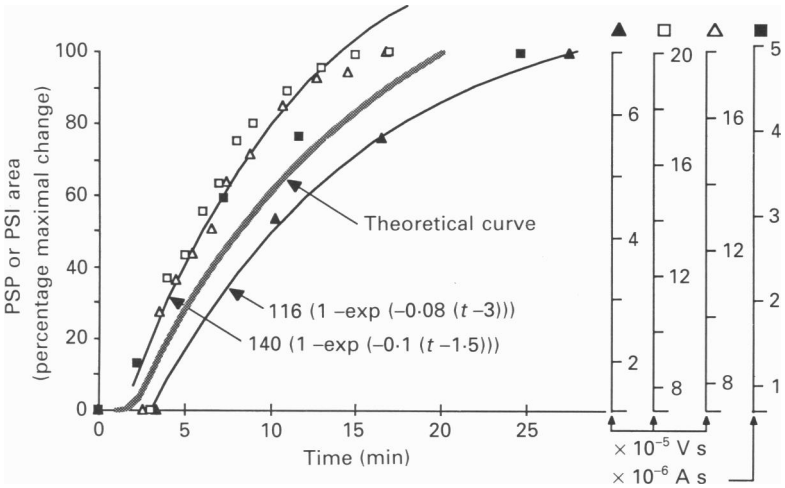

Fig. 10. The time course of synaptic facilitation by CaM kinase II in four experiments (absolute scales shown at right). Two empirically determined exponential curves (thin continuous lines) which enclose the entire data range were calculated. Parameters for the theoretical facilitation model were adjusted so the resulting inhibition curve would fall in the centre of the data range (thick stippled line).

5 units except for compartments C_{-2} through C_2 which were 'filled' with 1000 units. The active zone was modelled as extending from compartments C_4 through C_{14}; these compartments were each filled with 10^4 vesicles at time 0 ($V_0 = 10^4$). This model produced an exponential rate of facilitation very similar to that observed experimentally. As was the case with the synapsin I inhibition model, however, this curve was affected by the extent to which response facilitation was allowed. Thus it was assumed that a finite number of vesicles in the pre-terminal can be made available for release; i.e. the size of the 'releasable' pool is limited. (The same effect would be achieved if the rate of vesicle release during depolarization is limited.)

Analysis of maximum rate of rise of postsynaptic response

If synapsin I and CaM kinase II affect synaptic transmission by modulating the number of vesicles available for release–without modifying the dynamics of the release process *per se*, one would *not* expect the rate of vesicle release to change as a function of time. In fact, it would be expected that the effect of CaM kinase II on the probability of release (P) would be independent of time, i.e. it would not affect the kinetics of transmitter release (N) (Katz, 1968). If this were the case, the amplitude of the PSP would increase, while the shape of the waveform would remain constant.

In order to determine whether synapsin I and CaM kinase II altered the release kinetics, the maximum rate of rise (MRR) of the postsynaptic response and the peak amplitude (R_{peak}) were determined for each response. The normalized maximum rate

of rise (NMRR) was then calculated for each response as MRR/R_{peak}. Note that if two waveforms are scalar multiples of each other, then their NMRR values should be equal. In two typical uninjected synapses, postsynaptic currents were measured in response to stimulus pulses between 25 and 40 mV and the NMRR values calculated. The stimulus series were repeated twice in one and three times in

TABLE 2. Mean normalized maximal rate of rise (NMRR) values (±S.D.) for experimental subgroups in which voltage or current was recorded

	Voltage recording				Current recording			
	Synapsin I		CaM kinase II		Synapsin I		CaM kinase II	
Time (min)	0	22·56	0	14·5	0	19·4	0	29·667
NMRR	0·825± 0·387	0·722± 0·286	0·320± 0·037	0·400± 0·130	0·629± 0·075	0·630± 0·057	0·841± 0·258	0·700± 0·076
N	11		2		5		3	
t	1·663		−1·212		−0·050		1·253	
P	0·127		0·439		0·957		0·337	

Mean times of post-injection recordings are as noted. Paired t test values for within-group comparisons and P scores are shown. No within-group mean differences were significant.

the other synapse. The mean NMRR values at each stimulus amplitude for the five stimuli series was calculated and plotted against stimulus amplitude. A linear regression coefficient of $R^2 > 0{\cdot}95$ was found with a slope of $-5{\cdot}1 \times 10^{-4}$ mV ms^{-1} mV^{-1}. NMRR values for the same stimulus amplitude were quite close in successive stimulus runs, although the mean NMRR was significantly different for the two synapses (0·015 ms^{-1} and 0·030 ms^{-1} at 30 mV respectively).

A similar analysis of NMRR was carried out for synapsin I and CaM kinase II injection experiments. For each experiment, the NMRR was calculated for a time immediately pre-injection and again at a point 15–30 min later after significant inhibition or facilitation had occurred. Since the shapes of the postsynaptic response waveforms differed depending on whether postsynaptic voltage or current was being measured, they were analysed separately. The results of NMRR analysis for sixteen synapsin I and five CaM kinase II experiments are shown in Table 2, in which the means of the pre- and post-injection response amplitudes are given along with the mean post-injection measurement times. Note that for CaM kinase II, the mean facilitation is only 200–300% due to elimination of some of the largest responses in which saturation occurred. Within each of the four experimental subgroups (synapsin I or CaM kinase II) × (voltage or current)), the mean values were not significantly different ($P > 0{\cdot}1$, paired t test).

All experiments in which postsynaptic voltage was measured were then compared using an unpaired t test, and similarly, comparisons were made between all groups in which current was measured. In neither case were any significant differences found ($P > 0{\cdot}1$). Note that although the mean for the synapsin I voltage measurements is considerably larger than that for CaM kinase II, the latter is based on only two experiments. Finally, linear correlation analysis of NMRR was performed in several experiments in which multiple time points were measured (cf. Figs 3 and 10). In no

case was a significant correlation between NMRR and time post-injection found. These results indicate that the kinetics of vesicle release were unaffected by synapsin I or CaM kinase II. On the basis of these data, we conclude that during the time course of a given postsynaptic response, the probability of release was modified uniformly by synapsin I and by CaM kinase II.

DISCUSSION

The major findings of these experiments are as follows: (1) the degree of inhibition of transmitter release by dephosphorylated synapsin I is well correlated with the degree of invasion of the protein along the length of the presynaptic terminal. (2) Tail-phosphorylated synapsin I and heat-treated synapsin I have no effect on release. (3) Inhibition by dephosphorylated synapsin I is reversible. (4) CaM kinase II facilitates synaptic release. (5) The shape of the postsynaptic response waveform is not affected by either synapsin I or CaM kinase II over the duration of the response. We conclude from these data that the dynamics of synaptic transmission, specifically the number of vesicles available for release, are probably regulated by the ratio of tail-phosphorylated to dephosphorylated synapsin I which is determined enzymatically by CaM kinase II.

Synapsin I

The experiments involving injection of phosphorylated and dephosphorylated synapsin I showed that the rates of blockade of synaptic transmission were highly correlated with: (a) the state of phosphorylation of the protein, (b) the site of injection and (c) the rate of movement of the protein through the terminal. When the protein injections were large enough to fill rapidly most of the active release zone, the times to onset of blockade were short. Conversely, when synapsin I was injected far from the release site, the onset of the block was delayed. These data suggest that synapsin I acts specifically at the active zones to affect release.

The injection procedures *per se* did not appear to interfere with any aspect of synaptic transmitter release, including the availability of transmitter or the calcium current. Rather, three sets of experiments suggest that the effect of synapsin I on transmitter release is specific and dependent on the structure of this molecule. First, injections of synapsin I in which the tail only or both the head and tail were phosphorylated had no effect on release. Second, injection of heat-treated synapsin I also failed to affect release. Third, injection of avidin, a basic protein similar in size and pI to synapsin I did not alter synaptic transmission. In all these experiments, the injected proteins completely filled the presynaptic terminal. Therefore it is necessary for the tail site of synapsin I to be in the dephosphorylated state for it to block transmitter release.

As an additional test of the ability of synapsin I to bind to intracellular elements and inhibit vesicle movement, phosphorylated or dephosphorylated synapsin I was introduced into extruded squid axoplasm and the effect on the movement of subcellular organelles monitored by video-enhanced microscopy (McGuinness, Brady, Gruner, Sugimori, Llinás & Greengard, 1987; McGuinness *et al.* 1989). Following the injection of dephosphorylated synapsin I, both orthograde and

anterograde flow were significantly reduced. Injection of synapsin I phosphorylated only at the head partially inhibited organelle movement, and synapsin I phosphorylated only at the tail lacked any inhibitory effect. Injected CaM kinase II, in the presence of calcium and calmodulin, prevented the inhibitory effect of synapsin I. Dephosphorylated synapsin I does not appear to directly inhibit the transport mechanism subserving organelle movement, since the organelle movement along microtubules at the edges of the axoplasm (where the cytoskeletal structure was sparse) was unmodified by synapsin I (McGuinness *et al.* 1989). These data are consistent with the hypothesis that synapsin I immobilizes or restrains vesicles and/or other organelles by cross-linking them to cytoskeletal elements and that this cross-linking can be modulated by CaM kinase II.

CaM kinase II

CaM kinase II is capable of increasing transmitter release by up to sevenfold (Figs 9 and 10), which indicates that it plays a decisive role in the release process. At this time we cannot exclude the possibility that CaM kinase II has some minor effect on the calcium channel. However, the results obtained would require an approximately 50% increase in calcium entry even if a fourth-order relationship between I_{Ca} and transmitter release is assumed. This is totally inconsistent with the present data, which shows no detectable change in I_{Ca} within the limits of a measurement error of $< 5\%$.

In the present experiments, we observed an increase in the maximum rate of rise (MRR) of the postsynaptic response following CaM kinase II injections, confirming earlier findings (Llinás *et al.* 1985). Here we investigated the MRR in more detail to determine if the shape of the response (which is dependent on vesicle release kinetics) also changed following presynaptic protein injections. The rationale for this analysis is as follows. The variable N_{jR} (eqn (2)), which represents the number of vesicles released from a given compartment in response to a given depolarization, may be represented more explicitly as a function of time from the onset of the stimulus; i.e.

$$N_{jR} = \int_{t=0}^{\infty} P(t)\,\mathrm{d}t,$$

where $P(t)$ represents the probability that a given vesicle will be released as a function of time after depolarization, and 'N' would be proportional to the number of vesicles available for release (Katz, 1968). Thus, doubling the number of available vesicles should, at least within certain limits, double the amplitude of the response. If $P(t)$ is unchanged, then the shape of the waveform should remain constant, depending only on N. In that case, then, the rate of change of response amplitude at any point on the curve should be proportional to the peak amplitude, and therefore the maximal rate of rise divided by the peak amplitude (NMRR) should be constant. This was in fact found when all successful injections of synapsin I or CaM kinase II were analysed either by comparing across experiments before and after injection, or within experiments as a function of time after injection. We conclude that these proteins do not alter dynamic aspects of vesicle release such as the duration of opening of ion channels or the rate of vesicle exocytosis. The most plausible mechanism, as initially suggested in a previous paper (Llinás *et al.* 1985) and

supported by *in vitro* studies (cf. Greengard *et al.* 1987), is that CaM kinase II acts to increase availability of synaptic vesicles by phosphorylating synapsin I. The ability of CaM kinase II to increase transmitter release from presynaptic terminals has recently been confirmed using rat brain synaptosomes (Nichols, Wu, Haycock & Greengard, 1989).

Model of preterminal protein diffusion, and of synaptic transmitter modulation by presynaptic protein injection

The simulations of postsynaptic inhibition and facilitation presented above were designed as a heuristic tool to test whether the observed rates of PSP inhibition and facilitation could be predicted by a unified model of vesicle release in which the amplitude of a PSP is dependent on phosphorylation of synapsin I by CaM kinase II. The data were, in fact, highly consistent with the model of release described by eqns (1) to (7) above. The compartmental model correctly describes the time courses of both inhibition by synapsin I and facilitation by CaM kinase II (eqns (7) and (8)). In both cases, limits on the number of vesicles available for release were included, and not found to affect the shape of the curves.

General hypothesis relating synapsin I to transmitter release: facilitation of transmitter release by calcium-dependent mobilization of synaptic vesicles

The ubiquitous nature of synapsin I in presynaptic terminals (DeCamilli *et al.* 1983), and the fact that its injection at the release site is capable of modulating transmitter release, raises the question of the mechanism by which synapsin I affects release. While we cannot exclude the possibility that synapsin I might be an integral part of the machinery for transmitter release itself, several facts argue against this view. First, if phosphorylated synapsin I were to directly promote vesicle release, one would expect that its injection would produce, following calcium entry, a continuous transmitter release leading to vesicle depletion and transmission failure. This was never observed. Furthermore, recent experiments failed to find any increase in miniature endplate potential frequency following such injections (Llinás, Sugimori, Lin, McGuinness & Greengard, 1988; Lin, Sugimori, Llinás, McGuinness & Greengard, 1990).

Another argument against synapsin I being a direct transmitter-release agent involves the time course of phosphorylation by CaM kinase II following calcium entry. The onset of transmitter release in the squid giant synapse begins as soon as 180 μs following calcium entry (Llinás *et al.* 1981*b*; Llinás *et al.* 1982) and peaks at about 1 ms. In contrast, the turnover rate for phosphorylation of synapsin I by CaM kinase II, calculated from data in McGuinness *et al.* (1985), is approximately 17 ms. It is thus difficult to see how this relatively slow phosphorylation reaction could produce the time course associated with a PSP, which is over within a few milliseconds.

Since synapsin I does not appear to be directly involved in vesicular release, we propose instead that it regulates the availability of vesicles for release. The biochemical and physiological studies noted above indicate that synapsin I restrains vesicles, probably close to the presynaptic release site, so that they cannot be released during depolarization. Calcium entry would thus trigger two events. First,

synaptic vesicles would be released, possibly by direct electrostatic shielding of negative charges by calcium or some other intermediate step. Second, a delayed effect independent of the release mechanism would occur after calcium had moved beyond the release site, by increasing the number of releasable vesicles following phosphorylation of synapsin I via activation of CaM kinase II. Physiological measurements indicate that the resting calcium conductance may have a powerful effect on the number of vesicles available at a given time (Simon, Sugimori & Llinás, 1984; Simon & Llinás, 1985). Indeed, resting calcium influx near the active zones may establish a steady-state level of phosphorylated synapsin I for regulation of vesicle availability close to the release site. The occurrence of an action potential would then increase the number of readily releasable vesicles by increasing the local calcium concentration and enhancing synapsin I phosphorylation. Such facilitation may underlie what has been considered to be calcium-dependent facilitation. This hypothesis is particularly attractive in the case of the squid giant synapse, as the large diameter of the preterminal would make it difficult to accumulate Ca^{2+} at the active zone.

This research was supported by Grant AFOSR850368 from the United States Air Force (R.L.) and MH 39327 (P.G.).

REFERENCES

AUGUSTINE, G. J. & CHARLTON, M. P. (1986). Calcium dependence of presynaptic calcium current and post-synaptic response at the squid giant synapse. *Journal of Physiology* **381**, 619–40.

AUGUSTINE, G. J., CHARLTON, M. P. & SMITH, S. J. (1985). Calcium entry into voltage-clamped presynaptic terminals of squid. *Journal of Physiology* **367**, 143–62.

AUGUSTINE, G. J., CHARLTON, M. P. & SMITH, S. (1987). Calcium action in synaptic transmitter release. *Annual Reviews* **10**, 633–693.

BAHLER, M. & GREENGARD, P. (1987). Synapsin I bundles F-actin in a phosphorylation-dependent manner. *Nature* **326**, 704–707.

BENFENATI, F., BAHLER, M., JAHN, R. & GREENGARD, P. (1989). Interactions of synapsin I with small synaptic vesicles: Distinct sites in synapsin I bind to vesicle phospholipids and vesicle proteins. *Journal of Cell Biology* **108**, 1863–1872.

BULLOCK, T. & HAGIWARA, S. (1957). Intracellular recording from the giant synapse of the squid. *Journal of General Physiology* **40**, 565–577.

CZERNICK, A. J., PANG, D. T. & GREENGARD, P. (1987). Amino acid sequences surrounding the cAMP-dependent and calcium/calmodulin-dependent phosphorylation sites in rat and bovine synapsin I. *Proceedings of the National Academy of Sciences of the USA* **84**, 7518–7522.

DECAMILLI, P., BENFENATI, F., VALTORTA, F. & GREENGARD, P. (1990). The synapsins. *Annual Review of Cell Biology* **6**, 433–460.

DECAMILLI, P., CAMERON, R. & GREENGARD, P. (1983). Synapsin I (protein I), a nerve terminal-specific phosphoprotein. I. Its general distribution in synapses of the central and peripheral nervous system demonstrated by immunofluorescence in frozen and plastic sections. *Journal of Cell Biology* **96**, 1337–1354.

DECAMILLI, P. & GREENGARD, P. (1986). Synapsin I: A synaptic vesicle-associated neuronal phosphoprotein. *Biochemical Pharmacology* **35**, 4348–4355.

GRAND, R. J. A., PERRY, S. V. & WEEKS, R. A. (1979). Troponin C-like proteins (calmodulins) from mammalian smooth muscle and other tissues. *Biochemical Journal* **177**, 521–529.

GREENGARD, P., BROWNING, M. D., MCGUINNESS, T. L. & LLINÁS, R. (1987). Synapsin I, a phosphoprotein associated with synaptic vesicles: possible role in regulation of neurotransmitter release. *Advances In Experimental Medicine and Biology* **221**, 135–153.

HACKETT, J. T., COCHRAN, S. L., GREENFIELD, L. J., BROSIUS, D. C. JR & UEDA, T. (1990). Synapsin I injected presynaptically into goldfish Mauthner axons reduces quantal synaptic transmission. *Journal of Neurophysiology* **63**, 701–706.

HAGIWARA, S. & TASAKI, I. (1958). A study on the mechanism of impulse transmission across the giant synapse of the squid. *Journal of Physiology* **143**, 114–137.

HUTTNER, W. B., DEGENNARO, L. J. & GREENGARD, P. (1981). Differential phosphorylation of multiple sites in purified protein I by cyclic AMP-dependent and calcium-dependent protein kinases. *Journal of Biological Chemistry* **256**, 1482–1488.

HUTTNER, W. B. & GREENGARD, P. (1979). Multiple phosphorylation sites in protein I and their differential regulation by cyclic AMP and calcium. *Proceedings of the National Academy of Sciences of the USA* **76**, 5402–5406.

HUTTNER, W. B., SCHEIBLER, W., GREENGARD, P. & DECAMILLI, P. (1983). Synapsin I (protein I), a nerve terminal-specific phosphoprotein: its association with synaptic vesicles studied in a highly purified synaptic vesicle preparation. *Journal of Cell Biology* **96**, 1374–1388.

KACZMAREK, L. K., JENNINGS, K. R., STRUMWASSER, I., NAIRN, A. C., WALTER, U., WILSON, F. D. & GREENGARD, P. (1980). Microinjection of catalytic subunit of cyclic AMP-dependent protein kinase enhances calcium action potentials of bag cell neurons in cell culture. *Proceedings of the National Academy of Sciences of the USA* **77**, 7487–7491.

KATZ, B. (1968). *The Release of Neuronal Transmitter Substances*. Charles C. Thomas, Liverpool.

KATZ, B. & MILEDI, R. (1967). A study of synaptic transmission in the absence of nerve impulses. *Journal of Physiology* **192**, 407–436.

KENNEDY, M. B. & GREENGARD, P. (1981). Two calcium/calmodulin-dependent protein kinases, which are highly concentrated in brain, phosphorylate protein I at distinct sites. *Proceedings of the National Academy of Sciences of the USA* **78**, 1293–1297.

KENNEDY, M. B., MCGUINNESS, T. & GREENGARD, P. J. (1983). A calcium/calmodulin-dependent protein kinase from mammalian brain that phosphorylates synapsin. I. Partial purification and characterization. *Journal of Neuroscience* **3**, 818–831.

LIN, J. W., SUGIMORI, M., LLINÁS, R., MCGUINNESS, T. & GREENGARD, P. (1990). Effects of synapsin I and calcium/calmodulin-dependent protein kinase II on spontaneous neurotransmitter release in the squid giant synapse. *Proceedings of the National Academy of Sciences of the USA* **87**, 8257–8261.

LLINÁS, R., MCGUINNESS, T., LEONARD, C. S., SUGIMORI, M. & GREENGARD, P. (1985). Intraterminal injection of synapsin I or calcium/calmodulin-dependent protein kinase II alters neurotransmitter release at the squid giant synapse. *Proceedings of the National Academy of Sciences of the USA* **82**, 3035–3039.

LLINÁS, R., STEINBERG, I. Z. & WALTON, K. (1976). Presynaptic calcium currents and their relation to synaptic transmission: voltage clamp study in squid giant synapse and theoretical model for the calcium gate. *Proceedings of the National Academy of Sciences of the USA* **73**, 2913–2922.

LLINÁS, R., STEINBERG, I. Z. & WALTON, K. (1981*a*). Presynaptic calcium currents in squid giant synapse. *Biophysical Journal* **33**, 289–321.

LLINÁS, R., STEINBERG, I. Z. & WALTON, K. (1981*b*). Relationship between presynaptic calcium current and postsynaptic potential in squid giant synapse. *Biophysical Journal* **33**, 323–352.

LLINÁS, R. & SUGIMORI, M. (1978). Double voltage clamp study in squid giant synapse. *Biological Bulletin* **155**, 454.

LLINÁS, R., SUGIMORI, M., LIN, J. W., MCGUINNESS, T. & GREENGARD, P. (1988). Effects of synapsin I and CAM kinase II on evoked and spontaneous transmitter release in the squid giant synapse. *Biological Bulletin* **175**, 307.

LLINÁS, R., SUGIMORI, M. & SIMON, S. M. (1982). Transmission by presynaptic spike-like depolarization in the squid *Loligo pealii* giant synapse. *Proceedings of the National Academy of Sciences of the USA* **79**, 2415–2419.

MCGUINNESS, T., BRADY, S. T., GRUNER, J. A., SUGIMORI, M., LLINÁS, R. & GREENGARD, P. (1987). Inhibition by synapsin I of membranous organelle movement in isolated squid axoplasm. *Society for Neuroscience Abstracts* **13**, 1239.

MCGUINNESS, T. L., BRADY, S. T., GRUNER, J. A., SUGIMORI, M., LLINÁS, R. & GREENGARD, P. (1989). Phosphorylation-dependent inhibition by synapsin I of organelle movement in squid axoplasm. *Journal of Neuroscience* **9**, 4138–4149.

MCGUINNESS, T., LAI, Y. & GREENGARD, P. (1985). Ca^{2+}/calmodulin-dependent protein kinase. II. Isozymic forms from rat forebrain and cerebellum. *Journal of Biological Chemistry* **260**, 1696–1704.

MARTIN, R. & MILEDI, R. (1986). The form and dimensions of the giant synapse of the squid. *Philosophical Transactions of the Royal Society* B **312**, 355–377.

MILEDI, R. & SLATER, C. R. (1966). The action of calcium on neuronal synapses in the squid. *Journal of Physiology* **184**, 473–498.

NAIRN, A. & GREENGARD, P. (1987). Purification and characterization of Ca^{2+}/calmodulin-dependent protein kinase I from bovine brain. *Journal of Biological Chemistry* **262**, 7273–7281.

NICHOLS, R. A., WU, W. C., HAYCOCK, J. W. & GREENGARD, P. (1989). Introduction of impermeant molecules into synaptosomes using freeze/thaw permeabilization. *Journal of Neurochemistry* **52**, 521–529.

PETERSON, G. L. (1977). A simplification of the protein assay method of Lowry *et al.* which is more generally applicable. *Analytical Biochemistry* **83**, 346–356.

PETRUCCI, T. C. & MORROW, J. S. (1987). Synapsin I: An actin-binding protein under phosphorylation control. *Journal of Cell Biology* **105**, 1355–1363.

SCHIEBLER, W., JAHN, R., DOUCET, J.-P., ROTHLEIN, J. & GREENGARD, P. (1986). Characterization of synapsin I binding to small synaptic vesicles. *Journal of Biological Chemistry* **261**, 8383–8390.

SIEGHART, W., FORN, J. & GREENGARD, P. (1979). Ca^{2+} and cyclic AMP regulate phosphorylation of same two membrane-associated proteins specific to nerve tissue. *Proceedings of the National Academy of Sciences of the USA* **76**, 2475–2479.

SIMON, S. M. & LLINÁS, R. R. (1985). Compartmentalization of the submembrane calcium activity during calcium influx and its significance in transmitter release. *Biophysical Journal* **48**, 485–498.

SIMON, S. M., SUGIMORI, M. & LLINÁS, R. (1984). Modeling of submembranous calcium concentration changes and their relation to rate of presynaptic transmitter release in the squid giant synapse. *Biophysics Journal* **45**, 264a.

TITUS, J. A., HAUGLAND, R., SHARROW, S. O. & SEGAL, D. M. (1982). Texas red, a hydrophilic, red-emitting flurophore for use with fluorescein in dual parameter flow microfluorometric and fluorescence microscopic studies. *Journal of Immunological Methods* **50**, 193–204.

UEDA, T. & GREENGARD, P. (1977). Adenosine 3′,5′-monophosphate-regulated phosphoprotein system of neuronal membranes. I. Solubilization, purification, and some properties of an endogenous phosphoprotein. *Journal of Biological Chemistry* **252**, 5155–5163.